Final Report

Period: 09/01/98 – 08/31/01

RTOP 622-44-79-20
NASA/Global Aerosol Climatology Project

# Investigations of Radiative Forcing of Indonesian Biomass Burning using GMS Radiance Measurements

by

Ming-Dah Chou
Laboratory for Atmospehres
NASA/Goddard Space flight Center

1. Objectives

The objectives of this research effort are to assess the direct effect of aerosols over global oceans on the Earth's radiation budgets and the impact on climate. Special effort has been directed toward the aerosols induced by the biomass burning in the Indonesian region.

2. Data Source and Approaches

The National Aeronautics and Space Administration launched the Sea-viewing Wide Field-of-view Sensor (SeaWiFS) satellite on 1 August, 1997 to measure global ocean color and to retrieve ocean bio-optical properties. The retrieved aerosol optical thickness and the Ångström exponent over global oceans is by-products of the SeaWiFS atmospheric correction for ocean color products . The aerosol data are available starting from September 1997. The SeaWiFS is a polar orbiting satellite with an equatorial crossing at local noon, and the temporal resolution of the retrieved aerosol optical thickness and Ångström exponent is once a day and has a high spatial resolution of 1 km at the nadir.

We conduct radiative transfer calculations and GCM simulations to assess the radiative forcing of aerosols retrieved from the SeaWiFS radiance measurements and the effect on climate. The effects of aeorsols on the solar radiation (or aerosol radiative forcing, ARF) at the top of the atmosphere (TOA), in the atmosphere, and at the surface are calculated using the radiation model of Chou and Suarez (1999). Calculations of clear-sky solar fluxes include the absorption of solar radiation by ozone, water vapor, $CO_2$, and $O_2$, scattering due to gases (Rayleigh scattering), and the absorption and scattering due to aerosols. Interactions among gas absorption, Rayleigh scattering, aerosol scattering and absorption, and surface reflection are explicitly included using the δ-Eddington approximation.

Data input to the radiation model for clear-sky flux calculations include vertical profiles of temperature, humidity, and ozone, the aerosol optical properties, and the albedo of the ocean surface. The temperature fields are taken from the National Centers for Environmental Prediction/National Center for Atmospheric Research (NCEP/NCAR) reanalysis (Kalnay et al., 1996). The column water vapor is taken from the Special Sensor Microwave/Imager (SSMI) retrievals of Wentz (1994). The column ozone amounts are taken from the TOMS retrievals (McPeters et al., 1998), which are climatological monthly-mean values.

The asymmetry factor, $g$, varies slightly with aerosol models and spectral bands. For the maritime aerosols, the variation of $g$ with wavelength is in the range 0.783 - 0.790. Therefore, we fix the value of $g$ at 0.786 in calculating ARF. The single-scattering albedo affects significantly

the ARF, especially at the surface. Over the vast oceanic regions, most of the aerosols are maritime in nature, and sulfuric aerosols can be assumed as typical over oceanic regions. For maritime sulfuric aerosols, the absorption is weak, and we fix the single-scattering albedo, $\omega_o$, at 0.9955 in the model calculations, which is practically non-absorbing. For aerosols in regions of active tropical forest fires and in the windward side of major deserts, the optical thickness is large. The absorption of solar radiation by these aerosols is strong. Due to lack of detailed information on the absorption property of oceanic aerosols, we assume that $\omega_o$=0.9955 and $g$= 0.786 for $\tau_o$<0.18 to represent maritime aerosols and $\omega_o$=0.9 and $g$ = 0.69 for $\tau_o$>0.3 to represent dusts from deserts and smoke from forest fires. For 0.18<$\tau_a$<0.3, $\omega_o$ and $g$ are interpolated linearly with $\tau_o$.

To understand the aerosol distribution over global oceans, we also have computed the global distribution of the divergence of wind. The wind field of the NCEP/NCAR reanalysis is used in this study. Finally, the clear-sky TOA flux derived from the Clouds and the Earth's Radiant Energy System (CERES) (Wielicki et al., 1996) is used for the comparison with the model-calculated clear-sky solar flux at TOA.

## 3. Aerosol radiative forcing

The aeerosol radiative forcing (ARF) at TOA and the surface averaged over the year 1998 are shown in Fig. 1. The ARF's are first calculated for each day and each 1˚x1˚ latitude-longitude region, then averaged over the year. Large aerosol cooling of the ocean-atmosphere system (upper panel) exceeding 6 W $m^{-2}$ is found in the tropical Atlantic, central equatorial Pacific, southern hemispheric high latitudes, and the coastal regions extending from East Africa, Arabian Sea, Bay of Bengal, Southeast Asia, to East Asia. In the eastern tropical Atlantic, the maximum cooling exceeds 8 W $m^{-2}$ due to aerosols from Sahara dust and forest fires. The minimum cooling is located in the subtropics, especially in the SH where the cooling is < 4 W $m^{-2}$.

The lower panel of Fig. 1 shows the annual-mean ARF at the surface. The distribution of ARF at the surface follows closely the ARF at TOA. In the tropical Atlantic and the Arabian Sea, the forcing at the surface is much larger than that at TOA, with a maximum cooling of ~15 W $m^{-2}$. By taking the difference between the forcing at TOA and the surface, it follows that aerosols in these regions enhance the solar heating of the atmosphere by ~4 W $m^{-2}$. It is noted that the large surface ARF in the tropical Atlantic and the Arabian Sea occurs primarily in the summer months of May-September, 1998.

The largest ARF occurs in the eastern portion of the tropical Atlantic and spread westward to the east coasts of Central America and northern South America. High ARF is found through

the whole year. The large aerosol forcing is expected to have a significant effect on cloud dynamics, the atmospheric stability, and the atmospheric circulation in the tropical Atlantic. In the Arabian Sea and the Indian Ocean, large aerosol forcing is found in the Spring and Summer (from March through September).

Table 1 shows the aerosol radiative forcing averaged over oceans in January, April, July, October, and the whole year of 1998. The seasonal change in ARF is large. The maximum and minimum of the monthly-mean ARF differ by ~33% in the Northern Hemisphere (NH) and ~50% in the SH. The seasonal variation of the incoming solar radiation at TOA is larger at high latitudes than at low latitudes. Because there is larger fractional oceanic coverage at high latitudes in the SH than in the NH, the seasonal variation of ARF in the SH is larger than the NH. Averaged over global oceans, the annual mean ARF is -5.4 W $m^{-2}$ at TOA and -5.9 W $m^{-2}$ at the surface. Aerosols enhance the atmospheric solar heating by 0.5 W $m^{-2}$.

During the 1997-1998 El Nino period, the big Indonesian fires produced a large amount of aerosols. Figure 2 shows that in October 1997 the ARF in the neighborhood of the maritime continents reaches -10 W/$m^2$ at TOA and -25 W/$m^2$ at the surface, with an enhanced atmospheric solar heating of 15 W/$m^2$. This large change in the atmospheric and surface radiation budgets over a large area is expected to have a significant impact on the regional and seasonal climate. Generally, the reduced surface heating due to aerosols will reduce the transfer of water vapor and latent heat to the atmosphere. The atmospheric boundary layer will be more stable and the atmospheric circulation is expected to be less rigorous. Since the big 1997-1998 Indonesian forest burning lasted for several months and covered a large area, it might have a similar effect as the excess cloud absorption of solar radiation in decelerating the hydrological cycle and in strengthening the drought of the region associated with the El Nino.

## 4. Comparison with CERES clear-sky solar flux

Errors are expected to occur in the model-calculated ARF due to uncertainties in the aerosol optical thickness, single-scattering albedo, and asymmetry factor, as well as the radiative transfer parameterization. It is desirable to compare model calculations with satellite-retrieved fluxes at TOA. The clear-sky TOA fluxes $F^{\downarrow}$ derived from the CERES on TRMM satellite covers a period of eight months, from January to August 1998. The data has a temporal resolution of 1 month and a spatial resolution of 2.5˚x2.5˚ latitude-longitude. The TRMM satellite is a polar-orbiting satellite with a low inclination angle. The CERES only retrieves TOA fluxes at middle and low latitudes between 40˚S and 40˚N. In Figure (3), we compare the model-calculated net downward clear-sky solar flux with that of CERES (CERES minus model) for

January 1998. As can be seen in the figure, the difference is generally within 3 W $m^{-2}$. Large discrepancy is found in the southern extra-tropics where the CERES-retrieved $F^{\downarrow}$ is smaller than that of model calculations by >6 W $m^{-2}$. Consider the uncertainty in both CERES-derived and model-calculated $F^{\downarrow}$, this difference can be considered as small.

5. GCM Simulations of Aerosol Climatic Impact

To assess the climatic impact of aerosols induced by the Indonesian biomass burning during the fall of 1997, the SeaWiFS-inferred optical thickness have being incorporated into the two versions of GCM developed at the Goddard Laboratory for Atmospheres. The second half of the year 1997 is in a strong El Nino phase. The Indonesian region was under the influence of subsiding branch of the Walker circulation. The dry condition enhance the intensity of forest fires which, in turn, is expected to have an impact on El Nino. This task is currently under way.

Publications:

Chou, M.-D., P.-K. Chan, M. Wang, 2001: Aerosol radiative forcing derived from SeaWIFS retrieved aerosol optical properties. Accepted *J. Atmos Sci*, Special GACP Issue.

Weaver, C. J., P. Ginoux, N. C. Hsu., M.-D. Chou, and J. Joiner: Radiative forcing of Saharan dust: GOCART model simulations compared with ERBE data. Accepted *J. Atmos Sci*, Special GACP Issue.

Table 1. Aerosol radiative forcing over oceans. Units: W $m^{-2}$.

| | Oct 97 | Jan 98 | Apr 98 | Jul 98 | Annual |
|---|---|---|---|---|---|
| | | | TOA | | |
| NH | -4.8 | -5.2 | -6.7 | -6.1 | -5.7 |
| SH | -6.1 | -6.6 | -4.2 | -3.9 | -5.2 |
| Global | -5.5 | -6.0 | -5.2 | -4.9 | -5.4 |
| | | | Surface | | |
| NH | -5.2 | -5.7 | -7.8 | -7.4 | -6.5 |
| SH | -7.0 | -7.2 | -4.4 | -4.1 | -5.7 |
| Global | -6.2 | -6.6 | -5.8 | -5.6 | -6.1 |

## Figure Captions

Figure 1. The model-calculated aerosol radiative forcing at the top of the atmosphere (upper panel) and at the surface (lower panel) averaged over the year 1998. Units are W $m^{-2}$.

Figure 2. Aerosol radiative forcing at the top of the atmosphere, at the surface, and in the atmosphere for the month of October 1997, when there were big forest fires in Indonesia. Units are W $m^{-2}$.

Figure 3. Differences between the CERES-retrieved clear-sky net downward solar flux at TOA and that calculated using a radiation model with aerosols (upper panel) and without aerosols (lower panel). Units are W $m^{-2}$.

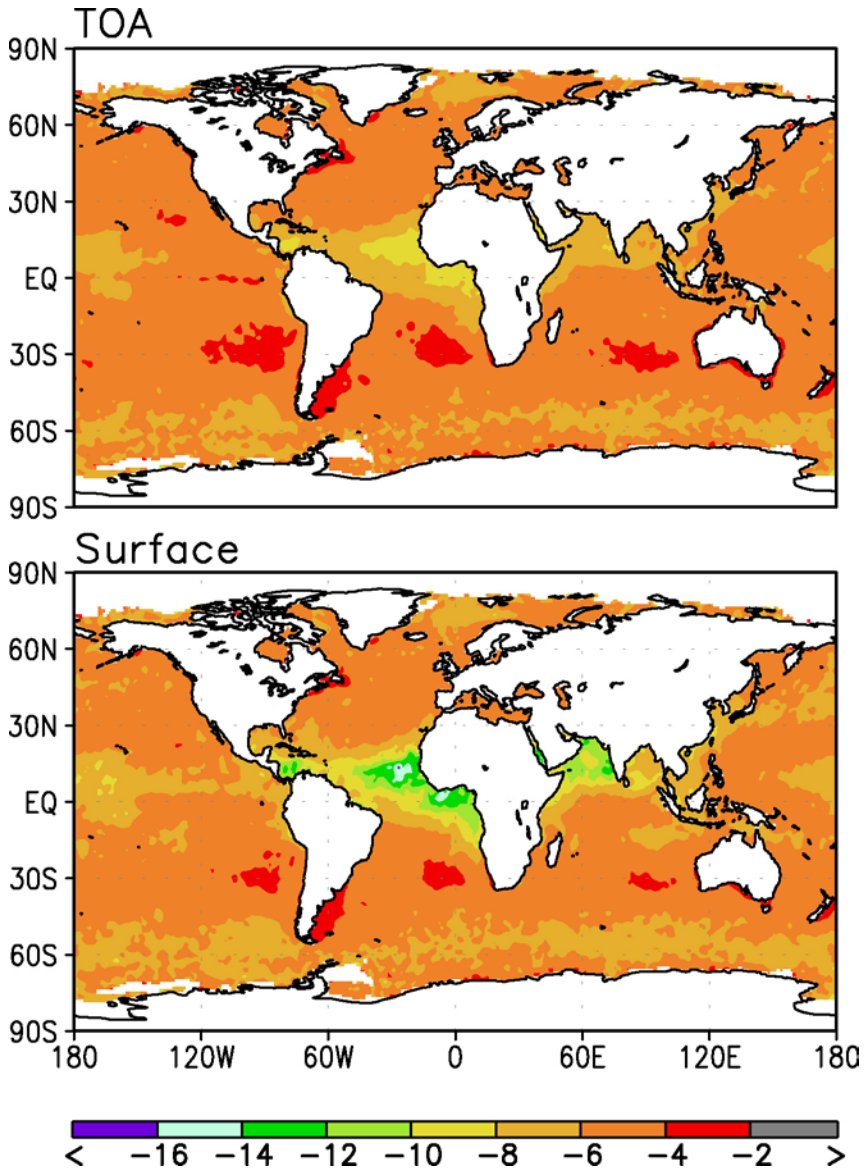


Figure 1. The model-calculated aerosol radiative forcing at the top of the atmosphere (upper panel) and at the surface (lower panel) averaged over the year 1998. Units are W $m^{-2}$.

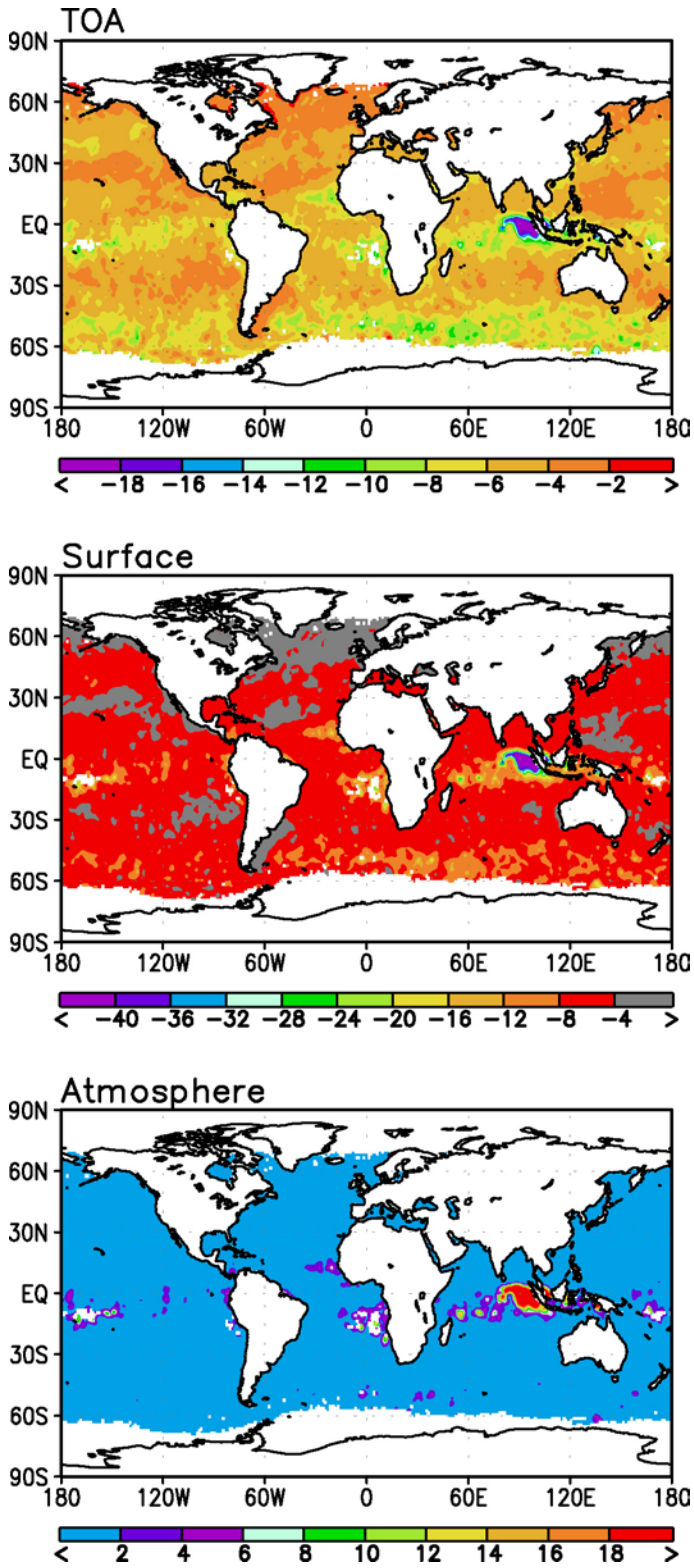


Figure 2. Aerosol radiative forcing at the top of the atmosphere, at the surface, and in the atmosphere for the month of October 1997, when there were big forest fires in Indonesia. Units are W $m^{-2}$.

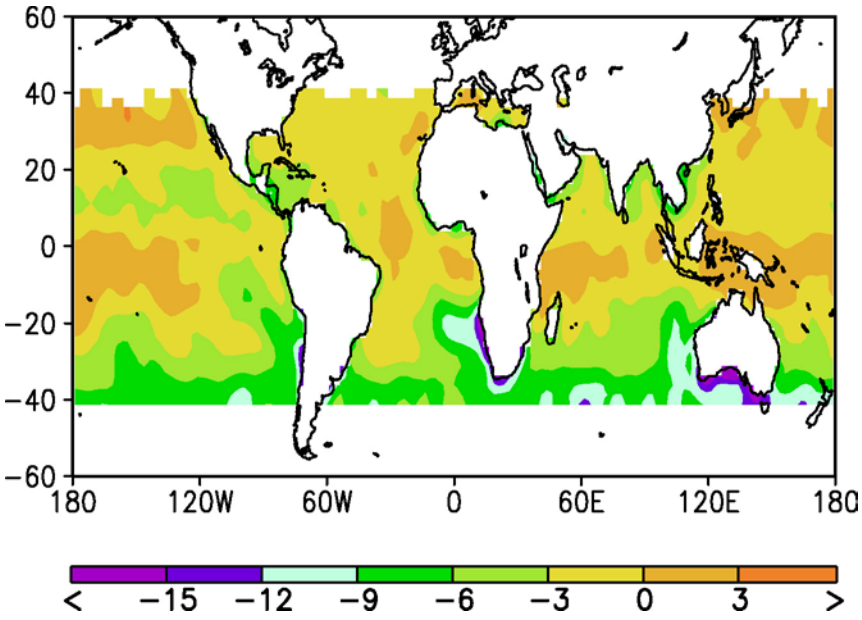


Figure 3. Differences in clear-sky net downward solar flux at TOA between that retrieved from CERES and that calculated using a radiation model with SeaWiFS-retrieved aerosols (CERES minus model) for January 1998. Units are W $m^{-2}$.